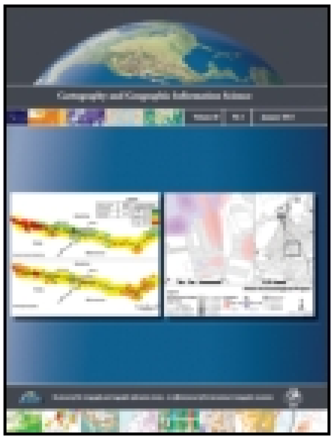

Cartography and Geographic Information Science
Publication details, including instructions for authors and subscription information:
http://www.tandfonline.com/loi/tcag20

Modeling the Potential Swath Coverage of Nadir and Off-Nadir Pointable Remote Sensing Satellite-Sensor Systems

Michael E. Hodgson & Bandana Kar
Published online: 14 Mar 2013.

CARTOGRAPHY AND GEOGRAPHIC INFORMATION SCIENCE

VOL. 35, NO. 3 JULY 2008

AN OFFICIAL JOURNAL OF THE CARTOGRAPHY AND GEOGRAPHIC INFORMATION SOCIETY
DEVOTED TO THE ADVANCEMENT OF CARTOGRAPHY IN ALL ITS ASPECTS

(PRINTED: ISSN 1523-0406)
(ONLINE: ISSN 1545-0465)

Research Papers

Cartography and Geographic Information Science

Published by
Cartography and Geographic Information Society
A member organization of ACSM
6 Montgomery Village Avenue, Suite 403, Gaithersburg, MD 20879
Tel: (240) 632-9716 * Fax: (240) 632-1321 * URL: http://www.cartogis.org
***CaGIS* Journal Managing Editor:** *Ilse Genovese*

Subscription: *CaGIS* Subscriber Services, P.O. Box 465, Hanover, PA 17331-0465, USA. Tel: (717) 632-3535; Fax: (717) 633- 8920; E-mail: mbaile@tsp.sheridan.com.

online *CaGIS***:** Register for online *CaGIS* at http://**www.ingentaconnect.com,** then follow instructions to activate your subscription.

Reprints: Sheridan Press, *Reprint Services*, P.O. Box 465, Hanover, PA 17331-0465, USA. Tel: (717) 632-8448, ext. 8134; Fax: (717) 633-8929; E-mail: lhess@tsp.sheridan.com.

* Cartography and Geographic Information Science (CaGIS) (ISSN 1523-0406) is published quarterly (January, April, July, and October) by the Cartography and Geographic Information Society, a member organization of the American Congress on Surveying and Mapping, 6 Montgomery Village Avenue, Suite 403, Gaithersburg, MD 20879. Periodicals postage paid at Gaithersburg, MD, and at additional mailing offices. Postmaster: Send address changes to Cartography and Geographic Information Science, Member Services, 6 Montgomery Village Avenue, Suite 403, Gaithersburg, MD 20879.

* The 2008 CaGIS journal basic subscription rates for institutions and non-member individuals are: $115 (USA) and $135 (international addresses). Annual printed and online subscription rates for institutions are: $180 (USA) and $200 (international). Institutional rates for online only subscriptions are: $160 (USA) and $180 (international). Individual non-member subscriber rates for printed and online CaGIS journal are: $130 (USA) and $150 (international). Individual online only subscription rates are: $115 (USA) and $135 (international). Back issues are sold to non-members at $20 per copy plus shipping and handling.

* All members of the Cartography and Geographic Information Society receive the CaGIS journal as part of their CaGIS membership dues. The journal subscription of $45 per year is part of membership benefits and cannot be deducted from annual dues.

* Manuscripts of research papers and technical notes should be sent to the Editor, **Elisabeth S. Nelson,** University of North Carolina–Greensboro, 3606 Birdsong Court, Summerfield, NC 27358, USA. Phone: 336-334-3896. E-mail: <**esnelso2@uncg.edu**>.

* Books for review should be sent to the Book Review Editor, c/o Ilse Genovese, Managing Editor, ACSM, 6 Montgomery Village Avenue, Suite 403, Gaithersburg, MD 20879. All other communication should be addressed to the Managing Editor by e-mail at <**ilse.genovese@acsm.net**>.

Modeling the Potential Swath Coverage of Nadir and Off-Nadir Pointable Remote Sensing Satellite-Sensor Systems

Michael E. Hodgson and Bandana Kar

ABSTRACT: Pointable sensor systems onboard many earth resources satellites today, particularly the higher spatial resolution sensors, provide for a near infinite set of collection opportunities. Satellite orbits of these systems are not systematic repetitive tracks. Predicting future collection opportunities requires predicting where the satellite will be and then computing the potential swath coverage from a pointable sensor along these orbits. While each agency or company models its own satellite-sensor systems, few publicly available sources exist for mapping future satellite ground tracks. Evaluating collection opportunities from multiple satellite-sensor systems from different agencies/companies is problematic. The purpose of the research described in this article was to develop a generic approach for modeling future satellite-sensor collection opportunities. In this article, formulae are developed for computing the potential swath coverage, and an algorithm is designed for constructing the potential swath coverage area. The solution to the swath coverage problem is based on spherical trigonometry, a well known map projection (i.e., azimuthal equidistant map projection) used in an unconventional dynamic form, and a satellite orbital propagation model. We demonstrate how the computation of the swath coverage area can be accomplished using a temporal series of re-centered map projections.

Introduction

Determination of the potential ground area imaged by a satellite-sensor system on future revisit dates was once a somewhat simple endeavor. Early earth resources satellites (e.g., Landsats 1-5 and 7, or the Defense Meteorological Satellites) carried sensor systems that only imaged in a nadir pointing fashion. Also, their orbital characteristics were such that their ground tracks were repetitive (e.g., the track sequence was repeated every 16 days). The familiar path-row maps (either hardcopy or the online web form) for the Landsat series, for example, were appropriate for such a stable, repetitive collection sequence. Such systematic orbits and nadir-only imaging allowed for elegant conic or cylindrical map projection solutions showing the ground-projected satellite tracks (Snyder 1987). Evaluation of *if* and *when* an area could be imaged by a specific satellite sensor were almost trivial.

The pointable sensor systems onboard many earth resources satellites, particularly the higher spatial resolution sensors (e.g., Quickbird 2, Orbview-3), provide a near infinite set of collection opportunities. The satellite orbits of these systems are not systematic repetitive tracks. They do not need to be repetitive as the sensors can point off-nadir and thus, "revisit" geographic locations. Predicting future collection opportunities requires predicting ***where*** the satellite will be and then computing the ***potential swath coverage*** from a pointable sensor along its orbit. While each agency or company models its own satellite-sensor systems, few publicly available sources (e.g., web sites) exist for mapping the future satellite ground tracks. Evaluating collection opportunities from multiple satellite-sensor systems is problematic. Those web sites offer, for the most part, very small-scale maps of future ground tracks, making precise, future collection opportunity predictions difficult. The goal of this research was to develop a generic approach for modeling future satellite-sensor collection opportunities.

Michael E. Hodgson and **Bandana Kar**, Department of Geography, University of South Carolina, Columbia, South Carolina 29208. Email: hodgsonm@sc.edu; kar@mailbox.sc.edu. Tel: 803-777-8976; Fax: 803-777-4972.

The problem studied here is the computation of a polygonal shape representing an area that may be imaged by a satellite with a pointable sensor on a single overpass. We refer to this as a *potential swath coverage area* in a 2-dimensional form and *potential swath coverage* in 1-dimensional form (Figure 1). The relevant sensor angles are instantaneous field of view (IFOV), field of view (FOV), and the maximum off-nadir angle of the pointable sensor. The ground-projected distances for these angles are pixel size (for instantaneous field of view), swath width (for field of view), and potential swath coverage (for the maximum off-nadir angle of the pointable sensor). The astrodynamics and lidar communities use the term *boresight angle* to refer to the off-nadir angle for which the FOV is

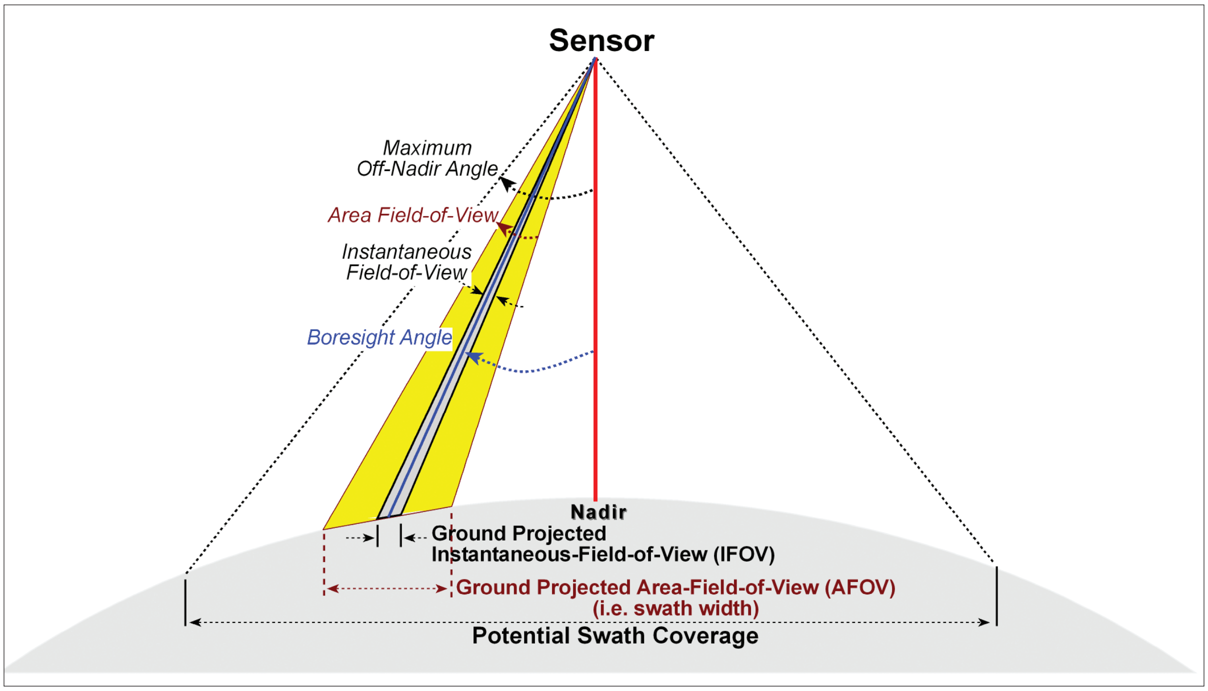

Figure 1. Profile view of the satellite-sensor, nadir, boresight angle, field-of-view, maximum off-nadir-angle and their projected forms on the Earth.

centered (Figure 1). The field of view is the angle that encloses the imaged area (e.g., analogous to the CCD array size or radar pulse width) (Jensen 2007). The instantaneous field of view is often reported, while the field of view is seldom reported but described in the ground-projected form as the swath width. The potential swath coverage, to our knowledge, is rarely derived or reported (Jensen 2007).

The parts of a complete solution to the problem presented here are:

1. Collect satellite-sensor viewing geometry possibilities (i.e., off-nadir and fore/aft angles);
2. Model the position (altitude, latitude, longitude, and heading) of satellite at times t_1 through t_2;
3. Determine potential visible swath below satellite position at times t_1 through t_2;
4. Integrate all potential visible swaths below multiple satellite positions along a path to form a potential swath coverage area; and
5. Map the potential swath coverage area with appropriate cartographic symbology (or analyze swath coverage polygon in a GIS context).

In this article, we develop 1) formulae for computing the potential swath coverage based on the field of view and satellite characteristics, and 2) an algorithm for constructing the potential swath coverage area based on the satellite position, heading, and potential swath coverage. Thus, we provide solutions for parts 3) and 4) above. This problem differs somewhat from the familiar image navigation problem where automatically registering the image is the goal (Salamonowicz 1986; Emery et al. 1989; Kelly et al. 1996; Rosborough et al. 1994; Emery et al. 2003). Our solution to the swath coverage problem is based on spherical trigonometry, a well known map projection, used in an unconventional *dynamic* form, and a satellite orbital propagation model. The accuracy of these solutions is dependent on modeling the location of the satellite via an orbital propagation model.[1] We demonstrate how the computation of the potential swath coverage *area* can be accomplished using a temporal series of re-centered azimuthal equidistance map projections. In addition, we demonstrate the error resulting from a spherical Earth assumption rather than an ellipsoidal Earth.

Azimuthal Equidistant Projection

A goal of the research described in this manuscript was to compute the polygonal area defining the satellite-sensor potential swath coverage

1 This orbital propagation problem is beyond the scope of this short article but may be investigated in the fundamental works by Hoots and Roehrich (1980) or Tapley et al.(2004).

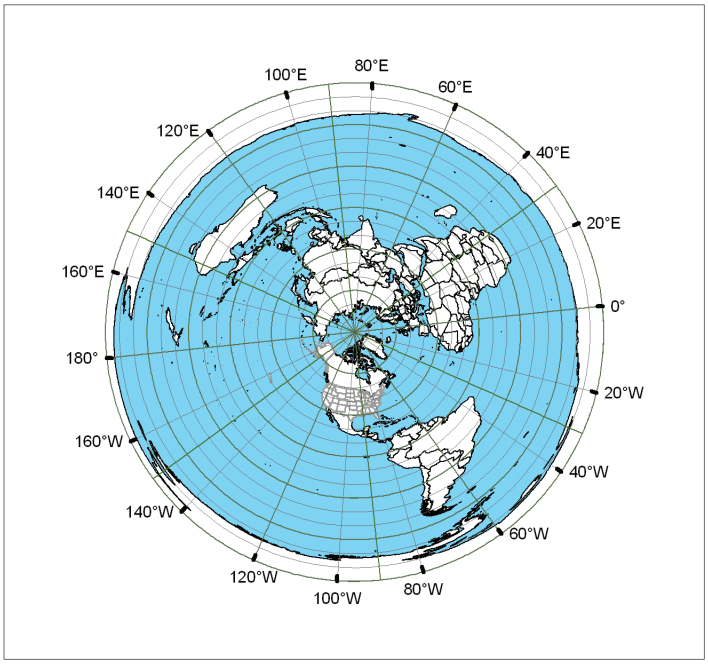

Figure 2. Example azimuthal equidistant map projection centered at the North pole.

area for mapping *or* GIS applications. In a GIS application, the map projection may be less important than the specific analytical technique utilized (e.g., point-in-polygon). For instance, determining if a ground location defined as a point is within the potential swath coverage area may be the primary objective. The paradox in this issue is that the analytical methods in modern GIS implementations almost always require the transformation of the spherical/ellipsoidal latitude and longitude coordinates to map projection coordinates before the analysis is performed. In this work, we focus on the accurate construction of the potential swath coverage polygon area and leave the selection of a map projection for later GIS applications to the user. An appropriate map projection is used in the process of constructing the potential swath coverage area.

In 1978, the Space Oblique Mercator (SOM) projection was developed for mapping the narrow band along the satellite ground track (Snyder 1978). In the SOM, the ground track is the only line on the map that is true to scale. The Satellite-Tracking projections (Snyder 1981) were developed in 1981 explicitly to show the satellite ground-tracks as straight lines. In the potential swath coverage area problem, however, the off-nadir (or across track) lines are also important and should be true to scale and with true direction. Further, being static map projections, the SOM or Satellite-Tracking projection would not be appropriate for computing a polygonal area that actually "wrapped" around the world, descending to the South pole, ascending to the North pole, and then descending again—repeatedly. These other map projections also do not meet the requirements of true scale along both the ground-track direction and off-nadir directions at the sub-satellite point.

The azimuthal equidistant map projection is proposed as an elegant solution to the problem of mapping the potential swath coverage and, subsequently, coverage area. This projection has been in use for more than 500 years, with the oldest recorded use in the 1500s (Snyder 1987, p. 191). It is most commonly used and recognized with a center at one of the poles (Figure 2). Snyder (1987) provides the computation of *x-y* coordinate positions for the azimuthal equidistant projection. For mapping the sensor swath coverage problem, we propose a solution that would center the projection at the sub-satellite location. Actually, we will use *multiple* sub-satellite locations and unique parameterized projections centered at each location along the satellite track. The individual swath coverage locations are then assembled to form the swath coverage area polygonal.

This azimuthal equidistant map projection has two properties that are particularly suited to the sensor coverage swath problem because they allow for a simple solution. These properties are:

- *Distances* measured from the *center* are true; and
- *Directions* from the *center* are true.

Computation of *x-y* coordinate positions for projections centered at the poles or equator are special cases and are described in Snyder (1987). Practically all remote sensing satellites are in an inclined orbit and never pass directly over the poles. For all other positions, the map coordinates on the sphere with radius R are derived as (Snyder 1987):

$$x = R\,k'\cos(\phi)\sin(\lambda-\lambda_0) \tag{1}$$

$$y = R\,k'\left[\cos(\phi_1)\sin(\phi)-\sin(\phi_1)\cos(\phi)\cos(\lambda-\lambda_0)\right] \tag{2}$$

The variable k' is derived from the ratio of the angular distance (c) of the point (ϕ, λ) from the map center and origin (ϕ_1, λ_0) to the sine of this angular distance:

$$k' = \frac{c}{\sin c} \tag{3}$$

$$c = \cos^{-1}\left[\sin(\phi_1)\sin(\phi) + \cos\phi_1\cos(\phi)\cos(\lambda - \lambda_0)\right] \quad (4)$$

The fundamental problem is a series of swath width calculations on the spherical Earth (Figure 3). Given a sub-satellite location (ϕ_1, λ_0) and satellite heading (direction satellite is moving to), the locations (ϕ, λ) perpendicular to the satellite heading are derived. The position on a planar Earth is easily computed from right triangles. However, at satellite altitudes the Earth cannot be considered planar. Thus, equations for deriving the swath width on a spherical Earth are introduced. Comparisons between spherical and ellipsoidal assumptions are shown.

Swath Coverage Algorithm

For nearly all satellite-sensor combinations, the potential swath coverage problem may be solved by the general algorithm in Table 1 with points defined in Figure 3. The sub-satellite locations along a track are derived from an orbital propagation model or computed as below. For each sub-satellite location, swath coverage positions perpendicular to the satellite heading are derived and then inverted from a centered azimuthal equidistant projection. The points defining the edges of the swath are derived from an off-nadir pointing angle. Finally, all swath coverage positions are assembled into a final polygon. By convention, the points may be assembled in a clockwise-fashion beginning at the earliest satellite time. For instance, the left-side (left of the satellite ground direction) points are ordered in descending latitude followed by the right-side points in an ascending latitude order. If large temporal swaths covering multiple hemispheres (e.g., east/west) are desired then ordering points simply by latitude is not applicable; ordering strictly by left-side and right-side of satellite heading is appropriate.

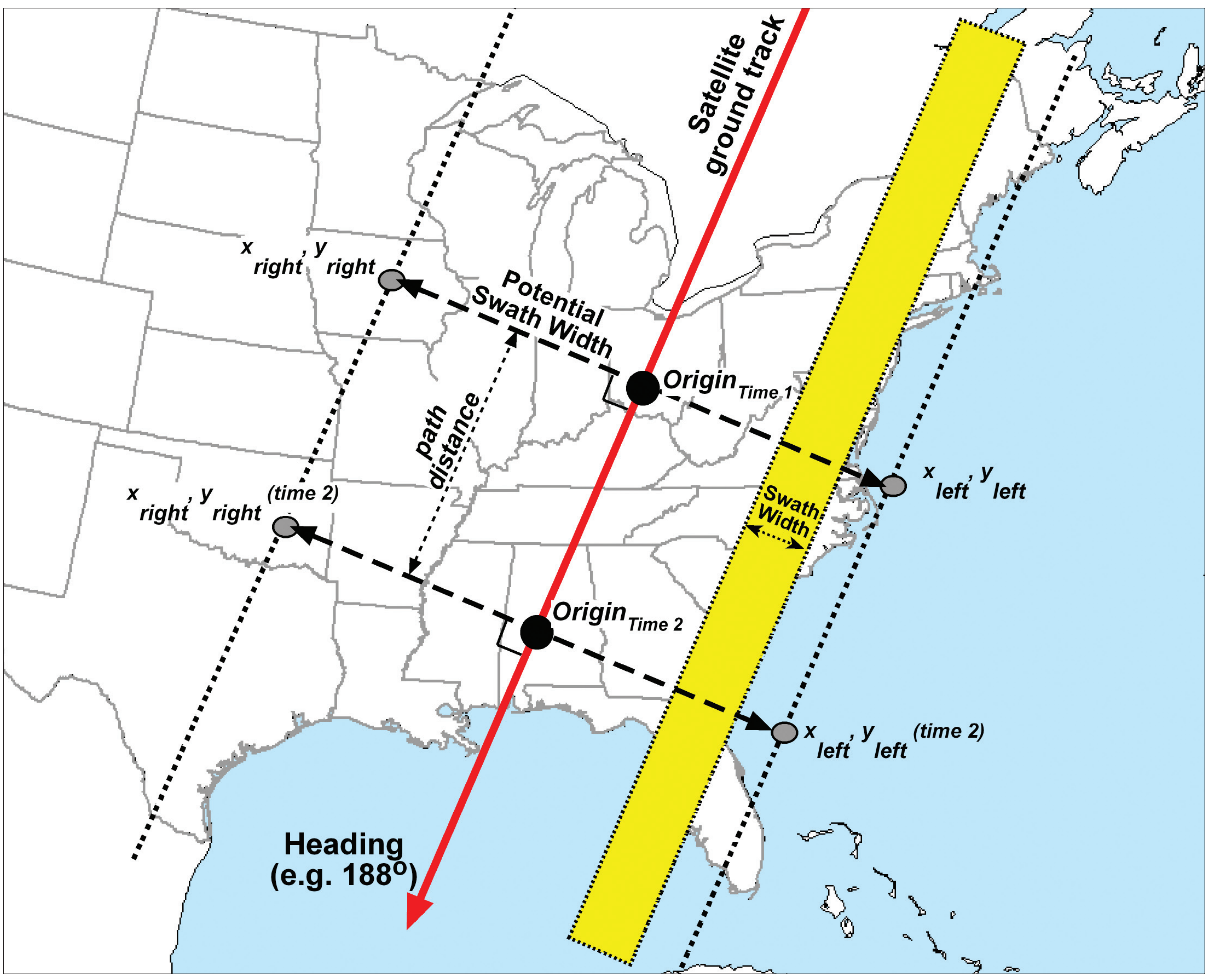

Figure 3. Azimuthal equidistant map projection centered at two sub-satellite locations (origin is 0, 0 for each) showing the satellite heading and potential swath coverage area.

For each sub-satellite location along a track,
Compute the sub-satellite location in geodetic coordinates
Center the azimuthal map projection at this sub-satellite location
Compute the visible locations in x-y space from the selected off-nadir angle
Invert the x-y location for geographic coordinates
Next sub-satellite location
Assemble the visible locations in a polygonal form

Table 1. Algorithm for deriving a potential coverage swath area.

Sub-satellite Location

Future (or even past) locations of the satellite may be derived from a satellite orbital propagation algorithm. Most orbital propagation solutions (Hoots and Roehrich 1980) are deterministic algorithms, although a few statistical solutions have recently been proposed (Tapley et al. 2004). Complete descriptions of these algorithms are beyond the scope of this article. Briefly, the deterministic algorithms require input data describing the location and characteristics of the Earth, moon, and solar bodies. The satellite ephemeris must also be provided. Many of the satellite orbital propagation algorithms will derive the geocentric location of satellite at a desired time (i.e., UTC). The accuracy of the algorithm is highly dependent on the age of the ephemeris. Geocentric locations must then be converted to geodetic locations for further mapping applications.

Planimetric Mapping Variables

The relevant parameters for mapping the potential swath coverage are satellite heading, altitude, sub-satellite location, and maximum off-nadir pointing angle (Figure 3). For general applications, the nominal altitude of the satellite may be used, and it is found in numerous textbooks or online sources. Otherwise, the altitude computed from the satellite orbital propagation algorithm is used. Satellite heading varies with latitude. The heading at the sub-satellite latitude is used to map the ground track at that location. Since the azimuthal equidistant map projection has the property that great circles are shown as straight lines, the ground-projected satellite track—were it not for Earth rotation during a satellite orbit—would also be a straight line. To map the potential coverage swath at that sub-satellite location, the maximum off-nadir angle is used to compute x_{left}, y_{left} and x_{right}, y_{right} (Figure 3).

By convention, the point x_{left}, y_{left} is left of the satellite *heading*. Most of the remote sensing satellites have a descending heading in a southwesterly direction (e.g., 188°) for daytime collections. Because the azimuthal equidistant map projection has the properties of true distances and directions from the center, computation of the "left" and "right" extremes of either the projected FOV or the maximum off-nadir angle is solved by rotating a point at the swath width distance from nadir (i.e., the center of the map projection).

Computation of the swath width or potential swath width locations may be derived by viewing the problem as a *2-dimensional* form. Since the swath characteristics are right angles from nadir (i.e., a 90-degree angle with the Earth's surface), the problem is 2-dimensional. To model the swath characteristics for a sensor that points both off-track <u>and</u> fore- or aft may require a 3-dimensional solution if the imaging time is precisely needed. Sensors pointing only off-track may be modeled in 2-dimensional form. In each example case described below, we use the boresight angle (s) to derive the swath width or potential swath coverage width. In practice, two angles (the extremes of the swath sides) would be used.

There are three fundamental approaches for computing the swath width on the surface: 1) planar surface assumption, 2) spherical assumption using intersecting lines, and 3) spherical assumption using an oblique triangle. For coarse high accuracy applications, solving the right triangle angle (Figure 4a) with a planar assumption may be sufficient:

$$swath\ width_m = \tan^{-1}\left(s_p\right) * \left(h\right) \tag{5}$$

For most applications, a spherical Earth model is desirable. One mathematical solution is to project a line from the satellite on the plane perpendicular to the Earth's surface. At this intersection point the subtended angle (a) between the intersection point, the Earth's center, and the satellite (Figure 4b) may be derived. The distance along this arc on the Earth's surface is simply:

$$swath\ width_m = \left(\frac{\alpha}{2\pi}\right) * R_e \tag{6}$$

The subtended angle (a) is solved from the intersection of lines.

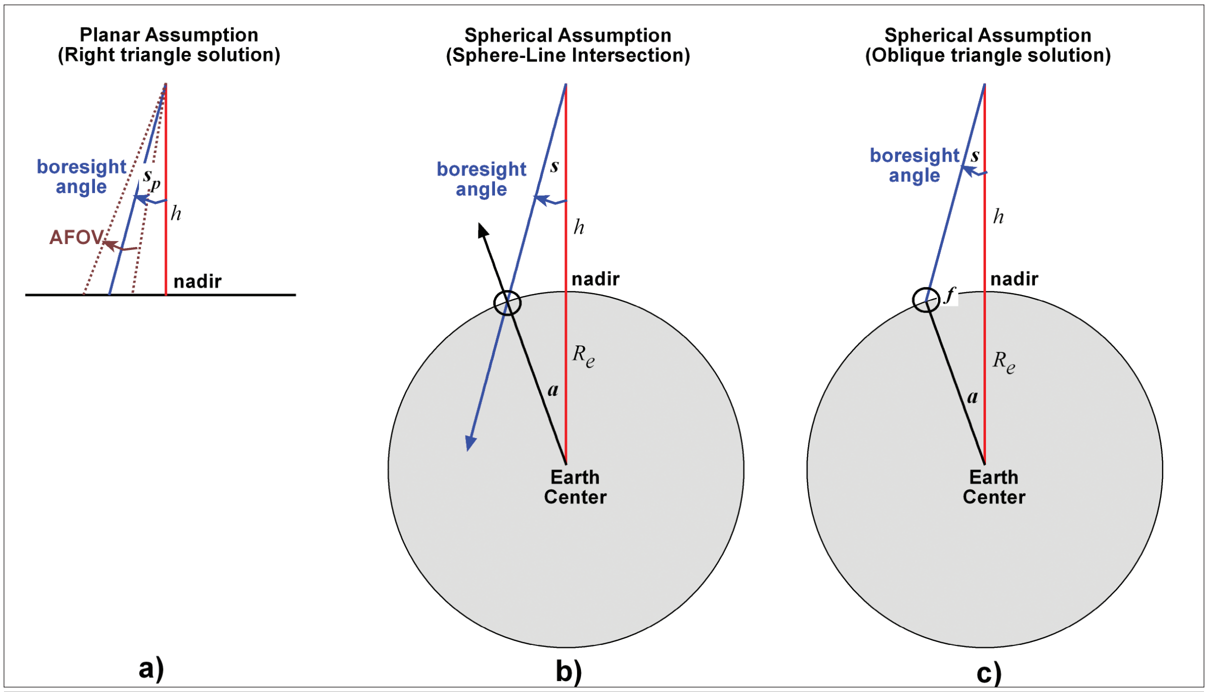

Figure 4. Three solutions for the swath width or potential swath width distance shown in profile view of a planar Earth (a) or spherical Earth in b) and c).

An alternate mathematical solution is to solve for the nonincluded angle (f) of an oblique triangle and, subsequently, the included angle (Figure 4c). The satellite altitude (h), Earth radius (R_e), and boresight angle (s) are known. The solution for f is based on the law of sines, which for this application is:

$$\frac{\sin(s)}{R_e} = \frac{\sin(f)}{R_e + h} \tag{7}$$

We can rearrange the terms to solve for the non-included angle f:

$$\sin(f) = \frac{\sin(s)(R_e + h)}{R_e} \tag{8}$$

The three angles (α, $\emptyset$, s) must sum to 180 degrees. Since $f = 180 - \alpha - s$, by substitution:

$$\sin(180 - \alpha - s) = \sin(\alpha + s) \tag{9}$$

and substituting $sin(\alpha + s)$ for $sin(f)$ in Equation (8):

$$\sin(\alpha + s) = \frac{\sin(s)(R_e + h)}{R_e} \tag{10}$$

Solving for α, we have:

$$\alpha = \sin^{-1}\left(\frac{\sin(s)(R_e + h)}{R_e}\right) - s \tag{11}$$

For example, if R_e = 6,378,137, h = 446,000, s = 5°, then α = .3506°. From Equation (6), the *swath width* is then 355,916.7m. Once the swath width is computed, the left and right positions on the azimuthal equidistant map projection at right angles to the satellite heading are:

$$x_{right} = \cos(heading - 180) * (-swath\ width_m) \tag{12}$$

$$y_{right} = -\sin(heading - 180) * (-swath\ width_m) \tag{13}$$

$$x_{left} = \cos(heading - 180) * (swath\ width_m) \tag{14}$$

$$y_{left} = -\sin(heading - 180) * (swath\ width_m) \tag{15}$$

Spherical vs Ellipsoidal

Ellipsoidal projections vary the size of the Earth's radius from the semiminor axis to the semimajor axis. For the WGS-84 ellipsoid, the

	Altitude at Apogee (meters)	Maximum Off-Nadir Angle (degrees)	Swath Width Major Axis 6,378,137 (meters)	Swath Width Minor Axis 6,356,752 (meters)	Difference (meters)
Landsat 7	703,000	7.4*	91,392	91,392	0
SPOT 5-HRG	826,000	27	428,522	428,550	28
Quickbird 2	446,000	30	261,828	261,840	12
Ikonos 2-OSA	679,000	45	721,275	721,443	168

*The Landsat 7 sensor does not point off-nadir. However, the maximum 'off-nadir' angle at the edge of the scene represents a 7.4^0 angle.

Table 2. Error in potential swath width using spherical vs. ellipsoidal form for AFOV.

semimajor axis is 6,378,137m while the semiminor axis is 6,356,752m. Potential swath widths using each of these radii for some common satellite-sensors are shown in Table 2. The swath width difference between a spherical and ellipsoidal projection is computed from the extremes in radii. As a percentage, the differences are all less than .02 percent. The greatest differences are with large off-nadir angles at high altitudes. Many commonly used sensors with shallower angles (e.g., 30° or less) exhibit differences less than 100m. Thus, for all but the most demanding mapping applications, the use of an ellipsoidal Earth model is not warranted (Snyder 1987, p. 185).

Potential Swath Polygon

Because the swath coverage area (see Figure 3) is derived from a series of centered map projections, the *x-y* coordinates for one projection are not compatible with the other centered projections along the satellite path. The latitude (ϕ) and longitude (λ) locations forming the polygonal area must be computed by inversion equations for each centered (at ϕ_1, λ_0) map projection (Snyder 1987):

$$\phi = \sin^{-1}\left[\cos(c)\sin(\phi_1) + \left(y \sin(c)\frac{\cos(\phi_1)}{p}\right)\right] \tag{16}$$

$$\lambda = \lambda_0 + \tan^{-1}\left[\frac{x\sin(c)}{p\cos(\phi_1)\cos(c) - y\sin(\phi_1)\sin(c)}\right] \tag{17}$$

Computing Path and Polygon

The ground-projected satellite path is constructed by computing the location of the satellite at multiple points in time and then generalizing the path as a series of straight-line segments between the points. The potential swath coverage area may be represented by a linked set of straight-line segments connecting the ground projected off-nadir locations (i.e., $x_{left\ i}$, $y_{left\ i}$ with $x_{left\ i+1}$, $y_{left\ i+1}$). Due to the convergence of latitudes at the poles, the resulting potential swath coverage polygon will be wider (in longitude degrees) at higher latitudes and narrower at lower latitudes (Figure 5), while the ground width (in meters) will be constant. For some applications (e.g., a single-scene purchase), only one sub-satellite point, altitude, off-nadir angle, and satellite heading will be known. Reconstructing the previous or latter sub-satellite locations may be performed for an ascending or descending path over a hemisphere[2] by extending the heading at the known sub-satellite location to earlier points ($X_{previous}$, $Y_{previous}$) in time (or later) using the azimuthal equidistant projection. An inversion of the $X_{previous}$, $Y_{previous}$ point from Cartesian to longitude-latitude is performed as with the off-nadir angle points above.

The Earth is rotating while the satellite is moving, resulting in a longitudinal shift of the sub-satellite point. Most of the high spatial resolution remote sensing satellites are moving at an approximate 7.5km/second ground speed, orbiting the Earth once every 90 minutes or so. Thus, the satellite path over an entire hemisphere only requires about 45 minutes of travel time. For descending satellites, the shift is west of the sub-satellite's previous longitude (or east of later time positions). The amount of rotation in longitude/sec for these high spatial resolution satellites is 0.00416° per second (or .25° per minute):

$$rotation^{\circ}_{\text{sec}} = \frac{360^0}{86,400} = 0.0041\bar{6} \tag{18}$$

[2] Extending the heading farther in time than a hemisphere assumes a simplistic satellite propagation model and neglects sun, moon, and perturbations in gravity effects. The positioning accuracy would deteriorate after a few Earth rotations.

Computing Earlier Sub-satellite Points

Reconstructing the previous or latter sub-satellite locations may be performed for an ascending or descending path over a hemisphere by extending the heading at the known sub-satellite location to later points in time (or earlier), using the azimuthal equidistant projection. An earlier sub-satellite point is computed as shown in Equations (19) and (20):

$$x_{previous} = \sin\left(heading_i + 180\right) * \left(path\ distance_m\right) \tag{19}$$

$$y_{previous} = \cos\left(heading_i + 180\right) * \left(path\ distance_m\right) \tag{20}$$

An inversion of the $X_{previous}$, $Y_{previous}$ point from Cartesian to longitude-latitude is then performed.

The angular rotation of swath width points must be altered for the new heading at earlier or later points. The heading for each sub-satellite point may be derived from the azimuth between the current sub-satellite point and the known sub-satellite point using the law of haversines:

$$y_h = \sin\left(\lambda_2 - \lambda_1\right)\cos\left(\phi_2\right) \tag{21}$$

$$x_h = \sin\left(\lambda_2 - \lambda_1\right)\cos\left(\phi_1\right) - \sin\left(\phi_1\right)\cos\left(\phi_2\right)\cos\left(\lambda_2 - \lambda_1\right) \tag{22}$$

$$heading_i = \tan_2^{-1}\left(y_h,\ x_h\right) \tag{23}$$

Mapping Actual Swath Coverage Area

The actual area field-of-view (AFOV) imaged by the satellite-sensor pointed at a given angle may be accomplished using similar logic as described for mapping the potential swath coverage area. For off-nadir pointing sensors, the resulting polygonal area will be a narrow strip within the potential swath coverage area (Figure 6). The points defining the edges of the swath are derived from an off-nadir pointing angle and the projected AFOV centered at the desired off-nadir pointing angle.

Temporal Series of Potential Swath Coverage Areas

The orbital period of most high spatial resolution remote sensing satellite systems is approximately 90 min. Thus, the Earth rotates approximately 23.75° longitude during this period. The resulting satellite tracks and potential swath coverage

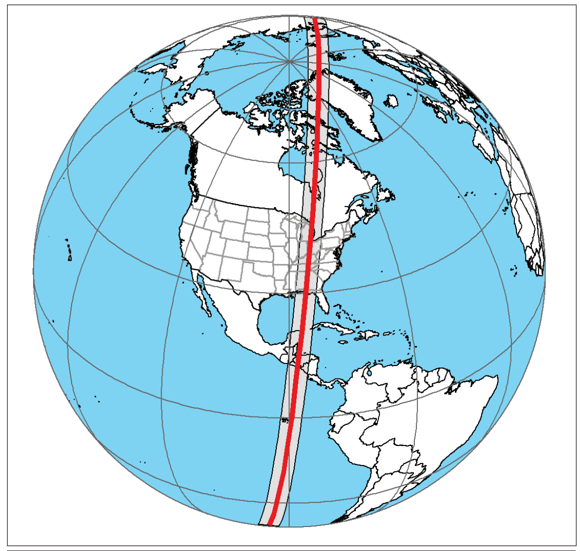

Figure 5. Example portion of a *potential swath coverage area* for Quickbird-2 using the maximum ±30-degree off-nadir sensor orientation and 188° heading from north. The satellite heading was projected ahead of and aft of the satellite position at 34° latitude, -85° longitude.

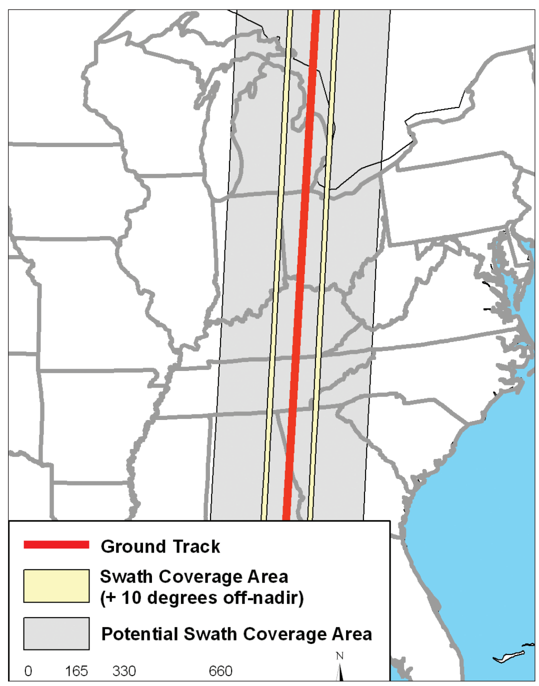

Figure 6. Example portion of a potential swath coverage area (±30° from orbital track) and projected swath widths at 10° either side of satellite track for Quickbird-2. Quickbird-2 operates on a 98° inclination (i.e., 188° heading on descending track) and has a nominal altitude of 446 km altitude.

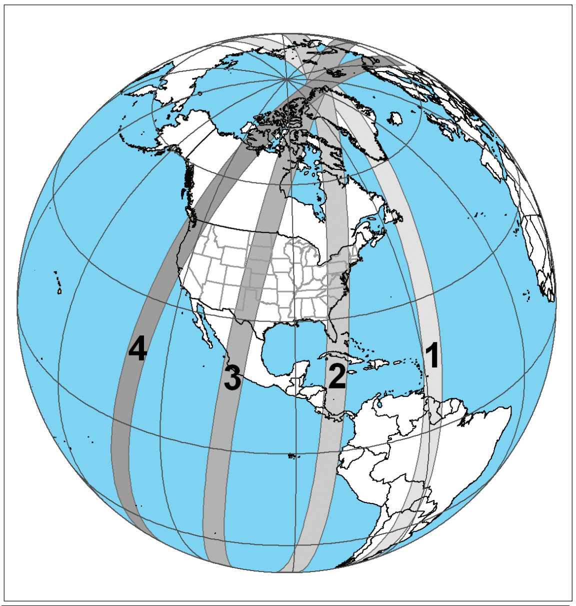

Figure 7. Example temporal series of potential swath coverage areas for Quickbird-2 daytime collections on September 27, 2007 over North America. Swaths are temporally numbered from earlier (1) to later times (2 through 4). Note the satellite is in a near-polar (~8 degree inclination) orientation with a 93.5minute orbital period.

area for Quickbird-2 are spaced 23.75° at the equator (Figure 7).

Conclusions

The post September 11 terrorism event resulted in initially highly restricted access to the satellite orbit ephemeris data. More recently, access to the ephemeris data through the U.S. Air Force has been relaxed, allowing for access by designated parties to this sensitive data. Such data are required for accurately modeling future satellite orbital tracks and the subsequent modeling of sensor viewing locations as described in this article.

The potential swath coverage model presented is appropriate for nearly all satellite-sensor combinations. Some sensors can image by pointing either forward (fore) or to the rear (aft) of the satellite direction of movement. Modifications may be needed for modeling fore/aft pointing sensors. The algorithm provided here can be used as is to determine the potential coverage area with only the off-nadir viewing angles. A slight geographic discrepancy will result from the Earth rotation between the forward pointing (or aft) imaging time and time when the satellite passes directly over the location. Constructing the potential coverage area polygon for the side-looking only radar (SLAR) sensors, such as RADARSAT, would require a modification to the polygon assimilation algorithm but not the swath coverage formulae. SLAR sensors do not image in a nadir fashion. They are side-looking only. Using the presented model to map the potential coverage areas would require mapping the potential area as described, and then removing the area in the restricted viewing angles. The potential swath coverage area model presented here has been implemented in a web-based spatial decision support system (SDSS). This SDSS, found at www.rshgs.sc.edu, was designed for use by DHS/FEMA and state emergency operations centers for predicting satellite image collection opportunities immediately after a disaster event.

The selection of the appropriate map projection for the display of either ground tracks or potential coverage polygons is grounded in the theoretical work on map projections used for other applications. Analyzing a potential swath coverage polygon in a GIS context is not so trivial. If using a "modern" GIS software package for analysis, the user must first project the data in a suitable map projection (or leave in latitude–longitude form, which is assumed to be a projected form). For large coverage polygons, such as those that span multiple hemispheres (e.g., east and west), the polygon appears to overlap itself when projected in a 2-D form (see Figure 7). One might argue that this overlap problem is due to the temporal nature of the viewing locations portrayed by the coverage area. However, even the clearly unique coverage area shown in Figure 5 will appear to overlap (i.e., back side of Earth with front side) itself in a 2-D map projected form. With either case, the apparently "overlapping" polygonal area results in analytical problems using a GIS designed for 2-D problems. Future research by others may help in studying global problems, even 2 ½-D form, from potential satellite coverage areas.

ACKNOWLEDGMENTS

We appreciate the contributions of Yang Cheng and Jim Miller in providing the satellite tracking algorithm. Comments by Sarah Battersby, John Jensen, Liz Nelson, and three anonymous reviewers were very helpful in revising an earlier version of this manuscript. This research was supported by a National Aeronautics and Space Administration (NASA) Earth Science Enterprise (ESE) Research, Education and Applications Solution Network cooperative agreement (REASoN #NCC-1303008).

REFERENCES

Emery, W.J., J. Brown, and Z.P. Nowak. 1989. AVHRR image navigation: Summary and review. *Photogrammetric Engineering and Remote Sensing* 55(8): 1175-83.

Emery, W.J., D. Baldwin, and D. Matthews. 2003. Maximum cross correlation automatic satellite image navigation and attitude corrections for open-ocean image navigation. *IEEE Transactions on Geoscience and Remote Sensing* 41(1): 33-42.

Hoots, F.R., and R.L. Roehrich. 1980. Spacetrack Report #3: Models for propagation of the NORAD element sets,.U.S. Air Force Aerospace Defense Command, Colorado Springs, Colorado.

Jensen, J.R. 2007. Remote sensing of environment: An Earth resource perspective. Upper Saddle River, New Jersey: Pearson Prentice Hall. 592 p.

Kelly, K.A., J.F. Hudson, and N. Pinkine. 1996. GOES-8 and -9 image navigation and registration operations. *SPIE* 2812: 777-88.

Rosborough, G.W., D.G. Baldwin, and W.J. Emery. 1994. Precise AVHRR image navigation. *IEEE Transactions on Geoscience and Remote Sensing* 32(3): 644-57.

Salamonowicz, P.H. 1986. Satellite orientation and position for geometric correction of scanner imagery. *Photogrammetric Engineering and Remote Sensing* 52(4): 491-9.

Snyder, J. 1978. The space oblique mercator projection. *Photogrammetric Engineering and Remote Sensing* 44(5): 585-96.

Snyder, J. 1981. Map projections for satellite tracking. *Photogrammetric Engineering and Remote Sensing* 47(2): 205-13.

Snyder, J. 1987. Map Projections: A Working Manual, USGS Professional Paper 1395 (United States Geological Survey: DC), 383 p.

Tapley, B.D., B.E. Schutz, and G.H. Born. 2004. Statistical Orbit Determination (Elsevier Academic Press: Burlington, Massachusetts).